Published June 5, 2006

Small GTPase Rab21 regulates cell adhesion and controls endosomal traffic of β1-integrins

Teijo Pellinen,[1,2] Antti Arjonen,[1,2] Karoliina Vuoriluoto,[1,2] Katja Kallio,[1,2] Jack A.M. Fransen,[3] and Johanna Ivaska[1,2]

[1]VTT Technical Research Centre of Finland, Medical Biotechnology, Turku FIN-20520, Finland
[2]University of Turku Centre for Biotechnology, Turku FIN-20520, Finland
[3]Department of Cell Biology, Nijmegen Center for Molecular Life Sciences, University Medical Center St. Radboud, University of Nijmegen, Nijmegen, Netherlands

Dynamic turnover of integrin cell adhesion molecules to and from the cell surface is central to cell migration. We report for the first time an association between integrins and Rab proteins, which are small GTPases involved in the traffic of endocytotic vesicles. Rab21 (and Rab5) associate with the cytoplasmic domains of α-integrin chains, and their expression influences the endo/exocytic traffic of integrins. This function of Rab21 is dependent on its GTP/GDP cycle and proper membrane targeting. Knock down of Rab21 impairs integrin-mediated cell adhesion and motility, whereas its overexpression stimulates cell migration and cancer cell adhesion to collagen and human bone. Finally, overexpression of Rab21 fails to induce cell adhesion via an integrin point mutant deficient in Rab21 association. These data provide mechanistic insight into how integrins are targeted to intracellular compartments and how their traffic regulates cell adhesion.

Introduction

Cell adhesion and migration are pivotal to many biological and pathological processes, including development, inflammation, repair, and cancer metastasis. The regulation of cell adhesion and motility is very complex. It requires the coordination of adhesion receptor–matrix interactions on the cell surface, trafficking of the receptors to and from the sites of adhesion (adhesion site turnover), and cytoskeletal reorganization inside the cell. Moreover, all these events have to be precisely orchestrated not only spatially but also temporally.

α/β-Integrin heterodimers are key molecules involved in cell adhesion and migration. Binding of cell surface–expressed integrins to specific ligands on the extracellular matrix is relatively well understood (Hynes, 2002). In contrast, much less is known about the turnover of integrin-containing adhesion sites and the intracellular traffic of integrins, although their importance in cell adhesion and migration is being increasingly recognized (Bretscher, 1996; Huttenlocher, 2005). In particular, the mechanisms that target integrins to specific endocytic compartments remain unknown.

Eukaryotic cells internalize cell-surface receptors by endocytosis. Integrins, like several other proteins lacking the AP-2 localization signal are internalized from the cell membrane via nonclathrin-derived structures, and some integrins have been shown to subsequently fuse with compartments containing clathrin-derived cargo proteins (Ng et al., 1999; Naslavsky et al., 2003; Upla et al., 2004; Weigert et al., 2004). The endocytosed receptors are subsequently recycled back to the cell surface or targeted for degradation. Depending on the cell type and the stimulus, integrins have been shown to be transported through caveolin-1–positive structures or early endosomes, either directly or via the perinuclear recycling compartment, back to the plasma membrane (Caswell and Norman, 2006).

Rab proteins are small GTPases that regulate both endocytosis and exocytosis. Several members have been implicated to function on the endocytic pathway, in which the function of Rab5 is understood in more detail (Miaczynska and Zerial, 2002). Rab5 regulates membrane traffic into and between early endosomes as well as vesicle transport along microtubules (Zerial and McBride, 2001).

Integrin traffic is regulated by several kinases (Ng et al., 1999; Roberts et al., 2001, 2003, 2004; Ivaska et al., 2002; Woods et al., 2004) and motor proteins (Zhang et al., 2004). However, very little is known about the mechanisms that target integrins to specific intracellular compartments and how this may be controlled. Although Rab proteins are known to bind a multiplicity of diverse effectors (Zerial and McBride, 2001), only a few examples demonstrate an interaction between a Rab GTPase and a cargo molecule (Seachrist et al., 2002; van IJzendoorn et al., 2002). We identify Rab21 and Rab5 as integrin-associated proteins and positive regulators of integrin traffic.

Correspondence to Johanna Ivaska: johanna.ivaska@vtt.fi

Abbreviations used in this paper: MVB, multivesicular body; Rluc, Renilla luciferase; shRNA, short hairpin RNA; TIRFM, total internal reflection fluorescence microscopy; WT, wild type.

The online version of this article contains supplemental material.

Supplemental Material can be found at:
http://jcb.rupress.org/content/suppl/2006/06/05/jcb.200509019.DC1.html

The Journal of Cell Biology, Vol. 173, No. 5, June 5, 2006 767–780
http://www.jcb.org/cgi/doi/10.1083/jcb.200509019

Published June 5, 2006

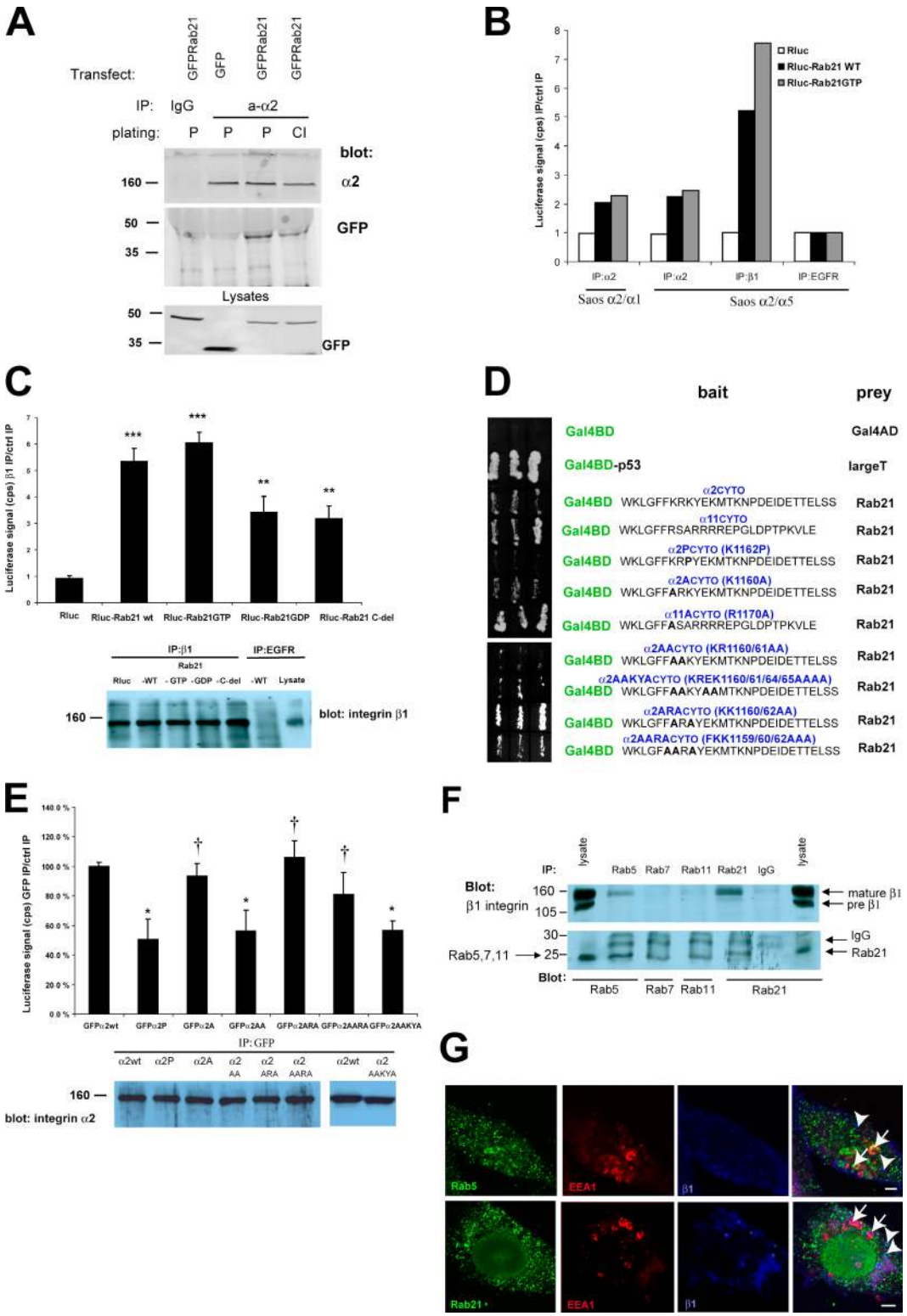

Figure 1. **Rab21 associates with cytoplasmic domains of α-integrin subunits.** (A) GFP-Rab21–transfected HeLa cells on plastic (P) or on collagen (CI; 1 h) were subjected to immunoprecipitations (IPs) with the indicated antibodies followed by blotting with anti-α2 or anti-GFP. (B and C) Full-length Rab21WT tagged with Rluc (Rluc-Rab21), mutants (Rluc-Rab21GTP, -Rab21GDP, or -Rab21C-del), or Rluc alone were expressed in Saos-2 cells stably expressing chimeric α-integrin subunits (α2/α1) or (α2/α5) (B) or HT1080 cells (C), and immunoprecipitation was performed with the indicated antibodies. The coprecipitated luciferase activity is presented relative to the basal nonspecific activity detected in the relevant control immunoprecipitations (anti-EGFR). Efficiency of the integrin immunoprecipitation was analyzed by Western blotting with anti-β1 from the same beads (means ± SD; $n = 5$; ***, $P < 7 \times 10^{-5}$; **, $P < 0.001$). (D) α2- and α11-integrin cytoplasmic domains and their point mutants (indicated in bold) were cloned as Gal4BD fusions and used as baits with Rab21 (amino acids 95–222) Gal4AD prey in yeast two-hybrid assays. Interaction between p53 and large T antigen was used as a positive control. (E) CHO cells were cotransfected with Rluc-Rab21 and GFP-α2 variants. Immunoprecipitation was performed with anti-GFP antibody, and the coprecipitated luciferase activity is presented relative to the activity detected in immunoprecipitations from α2WT-expressing cells.

Published June 5, 2006

Results

Identification of β1-integrins as Rab21-associated molecules

To identify novel integrin-interacting proteins, we screened a mouse embryonic cDNA library using α2-integrin cytoplasmic domain as bait in a yeast two-hybrid screen. The bait comprised the conserved membrane-proximal sequence shared by most α-integrin subunits followed by the α2-specific segment. Several positive clones encoded the COOH-terminal part of Rab21. Rab21 is a ubiquitously expressed and poorly characterized member of the Rab family that has recently been shown to function on the endocytic pathway (Simpson et al., 2004).

The ability of Rab21 to associate with integrins was further confirmed in human cells. GFP-tagged Rab21 coprecipitated with α2β1-integrin, a collagen binding molecule (Takada and Hemler, 1989), in cells plated either on collagen or on plastic (Fig. 1 A), indicating a constant, rather than a matrix adhesion–inducible, association between the two proteins. Furthermore, Rab21 was found to associate with several α/β1-integrin heterodimers. Rab21 coprecipitated with chimeric integrins containing the extracellular domain of α2-integrin fused to the cytoplasmic domains of either α1- or α5-integrin (Fig. 1 B) and endogenous integrins that were immunoprecipitated with antibodies against α1, α2, α5, α6, and β1 subunits (Fig. 1, B and C; and Table S1, available at http://www.jcb.org/cgi/content/full/jcb.200509019/DC1). These data suggest that the association involves the shared conserved membrane-proximal segment present in most α-subunit cytoplasmic domains. To get evidence for the association with an independent method, we performed yeast two-hybrid studies with α-tail mutants. In remating tests, we found that the COOH-terminal part of Rab21 (amino acids 95–222) was able to associate with the cytoplasmic tails of α2- and α11-integrin (Fig. 1 D). Introduction of a proline residue adjacent to the conserved membrane-proximal sequence (α2P, to create a conformational change into the α2 tail) markedly weakened the association between the α2 cytoplasmic domain and Rab21, whereas mutagenesis of a conserved positive charge in α2A (K1160) and α11A (R1170) tails had no effect (Fig. 1 D). To further characterize the Rab21–integrin association, we generated several mutants of α2-integrin. All of these mutants were expressed and mediated adhesion to collagen in transiently transfected CHO cells (Fig. 1 E and not depicted; see Fig. 6 E). Mutagenesis of residue R1161 (in α2AA and α2AAKYA, removing another conserved charged residue) to alanine significantly reduced α2 tail association with Rab21 judged by yeast mating tests and immunoprecipitations (Fig. 1, D and E). In addition, F1159A mutation (α2AARA, possibly creating a conformational change) showed reduced association in the yeast assays, whereas in immunoprecipitations the reduction was not significant. These data on the mutant integrins suggest that the conformation of the cytoplasmic domain and residue R1161 of α2-integrin are important for the Rab21 association. Finally, endogenous β1-integrins readily associated with endogenous Rab21 and to some extent Rab5 proteins in vivo. These associations were specific, as Rab7 and Rab11 failed to coprecipitate β1-integrin from these cells, even though separately all proteins were efficiently immunoprecipitated (Fig. 1 F).

Next, we studied the enzyme activity dependence of the association between integrins and Rab21. A Rab21 mutant (Simpson et al., 2004) that has defects in GTP hydrolysis (Rab21 Q76L, designated Rab21GTP) showed a 10–73% increase in its ability to associate with integrins in different cell lines when compared with Rab21 wild type (WT). In contrast, a mutant having defects in the binding of GTP (Rab21 T31N, designated Rab21GDP) showed a 26–35% decrease (Fig. 1, B and C; and Table S1). In addition, Rab21 with a deletion in the COOH terminus (Rab21c-del; residues 1–144) demonstrated inefficient association with the β1-integrins in vivo (37 ± 10% decrease; Fig. 1 C and Table S1).

Rab21 regulates the subcellular localization of β1-integrins

The cellular localization of endogenous β1-integrins, Rab5A, and Rab21 was studied in MDA-MB-231 cells. β1-Integrin was detected by the NH2-terminally binding antibody in the lumen of endogenous Rab5- and Rab21-positive large vesicles (Fig. 1 G, arrowheads). In addition, these cells also harbor large endogenous EEA1-positive endosomes that stained positive for Rab5A but showed very limited overlap with Rab21 (Fig. 1 G, arrows). α/β1-Integrin heterodimers can be expressed in active (extracellular domain detected by a monoclonal antibody HUTS21; active-β1 antibody) and inactive forms on the cell surface (extracellular domain of both forms detected by P5D2; pan-β1 antibody; Lenter et al., 1993; Luque et al., 1996). Expression of Rab21 in MDA-MB-231 breast cancer cells altered the subcellular localization of the total pool of β1-integrins. Cells expressing GFP-Rab21 contained numerous β1-integrin–positive vesicles (compare the nontransfected cell [Fig. 2 A, asterisk] and the transfected cell [Fig. 2 B]). The majority of these had GFP-Rab21 on their limiting membrane (72 ± 8% of pan-β1–positive vesicles and 68 ± 10% of active-β1–positive vesicles; $n = 20$ cells; Fig. 2, B and C). The recruitment of integrins to Rab21-positive intracellular structures was confirmed using two additional antibodies recognizing active-β1-integrin (12G10 [Mould et al., 1995] and P4G11 [Wayner et al., 1993]; Fig. 2, J and K). Similar to previous observations on breast cancer cells (Ng et al., 1999), the ECM proteins collagen and fibronectin were also detected in the endocytic structures (Fig. 2 L and not depicted). Interestingly, both Rab21 mutants induced marked alterations in the cellular distribution of β1-integrins. GFP-Rab21GTP showed a tubular-vesicular staining pattern that largely overlaps with the ER (Fig. 2, D and E; and not depicted), and active-β1-integrin

Efficiency of the integrin immunoprecipitation was analyzed by Western blotting with anti-α2 from the same beads (means ± SD; $n = 5$; *, $P < 0.05$; †, not significant). (F) Endogenous proteins were immunoprecipitated from MDA-MB-231 cells using the indicated antibodies and blotted with anti-β1 or anti-Rab antibodies. Shown is a representative experiment of five with similar results. (G) Nontransfected MDA-MB-231 cells were analyzed with three-color immunofluorescence staining (Rab5 or Rab21, green; EEA1, red; and β1-integrin, blue). Shown are 1-μm confocal sections. Arrows point to EEA1 and arrowheads to β1-integrin–positive vesicles. Bar, 5 μm.

Published June 5, 2006

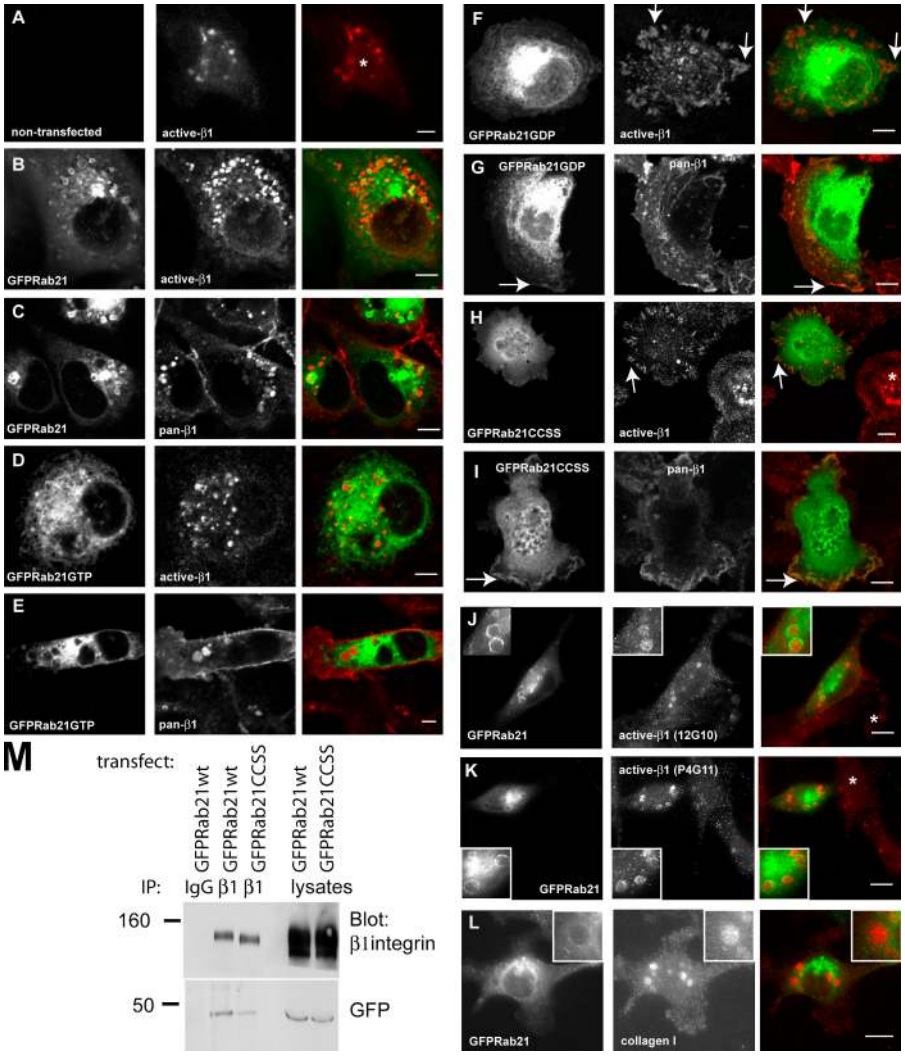

Figure 2. **Rab21 influences the subcellular distribution and traffic of β1-integrins.** (A–L) Nontransfected MDA-MB-231 cells (A) or MDA-MB-231 cells transiently expressing GFP-tagged Rab21 variants (B–L) plated on collagen were stained with pan-β1-integrin mAb (P5D2), active-β1 mAbs (HUTS-21, 12G10, or p4G11) or collagen type I pAb. Shown are 1-μm confocal sections. Asterisks indicate nontransfected cells, arrows point to prominent focal adhesions (F and H) or membrane localization (G), and insets show higher magnification (J–L). Bars, 10 μm. (M) Immunoprecipitation (IP) was performed with anti–β1-integrin mAb or control mouse IgG from GFP-Rab21WT– or -Rab21CCSS–transfected MDA-MB-231 cells followed by Western blotting with anti-β1 or anti-GFP. Equal amounts of lysates were loaded on the gel to control for transfection efficiency.

was detected in smaller and more irregularly shaped endocytotic integrin vesicles, whereas the pan-β1 antibody detected β1-integrin at the membrane, diffusely in the cytosol and accumulated in the large vacuolar structures. Strikingly, expression of GFP-Rab21GDP induced localization of active-β1 into large focal adhesions (Fig. 2 F, arrows), which are rarely detected in these highly motile cells endogenously (Fig. 2 A). GFP-Rab21GDP variant but not GFP-Rab21GTP was also seen at membrane ruffles (Fig. 2 G, arrows).

Proper membrane targeting of Rab21 was also mandatory for the regulation of integrin localization in vivo. Mutagenesis of the putative COOH-terminal prenylation motif (CCXXX; Opdam et al., 2000) in Rab21 resulted in a complete loss of vesicular localization of Rab21 (GFP-Rab21CCSS; Fig. 2, H and I) and a 55–62% ($n = 2$) less efficient association with β1-integrins as compared with the Rab21WT (Fig. 2 M). Cells transfected with GFP-Rab21CCSS showed prominent focal adhesions (active-β1 antibody; Fig. 2 H, arrows) when compared with the vesicular pattern observed in the nontransfected cells (Fig. 2 H, asterisk). Interestingly, these effects on integrin distribution were almost indistinguishable from that of Rab21GDP mutant (see the previous paragraph).

Rab21 regulates integrin traffic and associates with the internalized β1-integrin

To analyze the dynamics of integrin internalization, we investigated the ability of different Rabs to coprecipitate surface-labeled integrin before and after internalization. Interestingly, Rab5 and Rab21 antibodies very weakly coimmunoprecipitated biotinylated ∼160-kD proteins located on the plasma membrane (Fig. 3 A, no internalization). After 15 min of internalization, Rab5/21, but not Rab7, associated with biotinylated plasma membrane–derived ∼160-kD protein (Fig. 3 A, internalization 15 min, lanes 1 and 2). Reimmunoprecipitation revealed that β1-integrin was present, possibly with other plasma membrane–derived proteins, in the biotinylated Rab5/21 coprecipitating fraction (Fig. 3 A, internalization 15 min, lane 3), indicating that integrins associate with Rabs mainly after internalization. Further colocalization and internalization studies showed that internalized β1-integrins originally traverse through the same compartment as transferrin but, subsequently, the integrin traffics into separate, mainly GFP-Rab21–positive vesicles that can also contain caveolin, whereas transferrin remains colocalized extensively with GFP-Rab5 (Fig. S1, available at http://www.jcb.org/cgi/content/full/jcb.200509019/DC1).

Published June 5, 2006

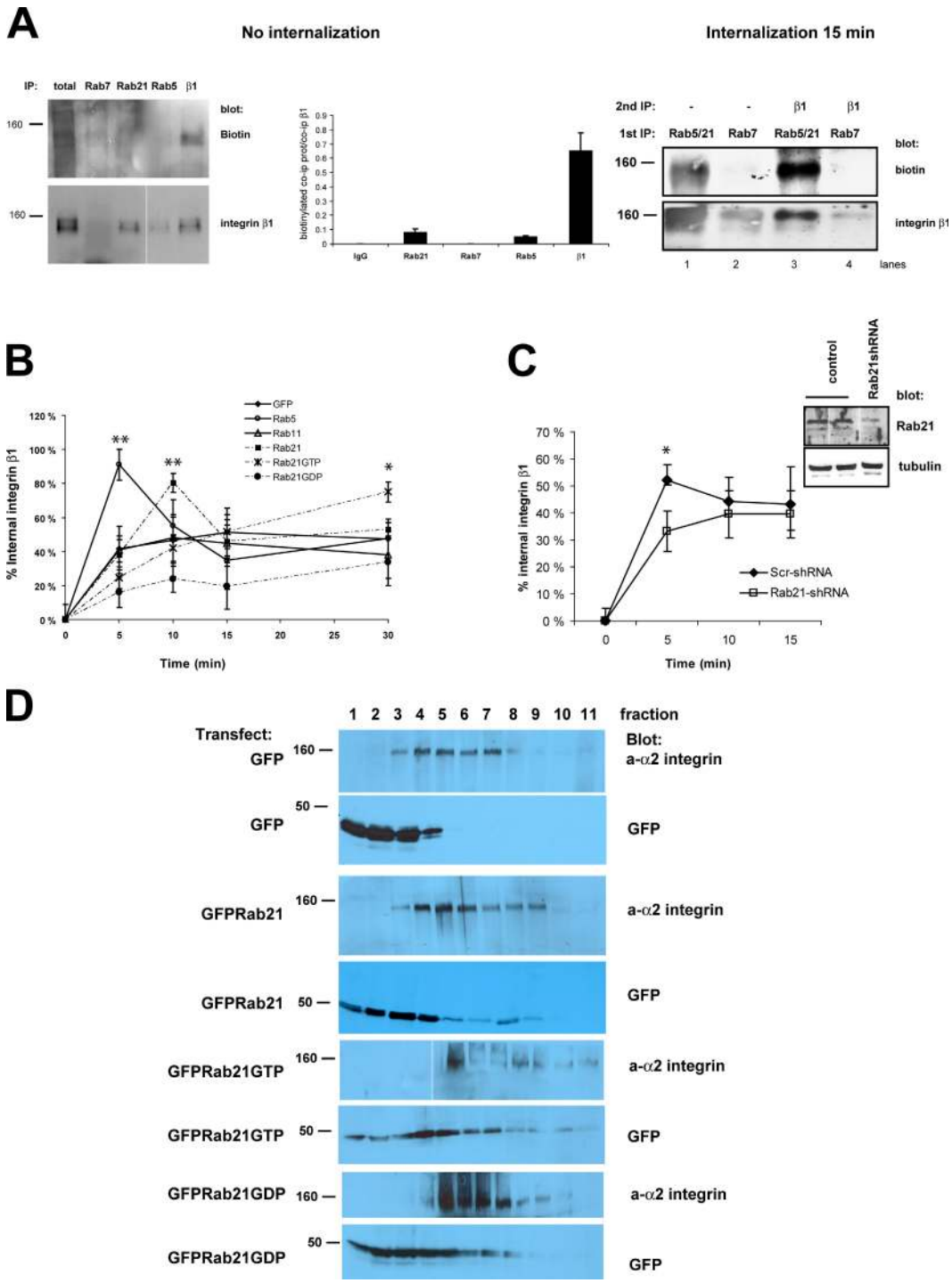

Figure 3. **Rab5 and Rab21 associate with β1-integrins after internalization and regulate integrin traffic.** (A) Nontransfected MDA-MB-231 cells were surface labeled with cleavable biotin and lysed immediately or allowed to internalize cell surface proteins for 15 min. Immunoprecipitations (IPs) were performed as indicated, and the Rab coprecipitating proteins were detected first with anti-biotin antibody followed by stripping and reprobing with anti–β1-integrin antibody. The quantification shows the amount of coprecipitated biotinylated protein relative to total precipitated integrin (means ± range; $n = 2$). (B and C) MDA-MB-231 cells transiently transfected with GFP or GFP-Rabs (B) or stably expressing Scr- or Rab21-shRNA (C) plated on collagen (1 h) and were surface labeled with cleavable biotin. Integrin traffic was allowed to for the times indicated, and biotin present on the cell surface was cleaved. The amount of biotinylated (intracellular) β1-integrin was determined with ELISA. The data are expressed as the percentage of internalized receptor relative to the total amount of cell surface–labeled integrin (means ± SD; $n = 5$; **, $P < 0.001$; *, $P < 0.05$). Shown are the pooled results of three experiments. Inset (C) shows the extent of Rab21 down-regulation in Rab21-shRNA–expressing cells. (D) GFP-, GFP-Rab21–, GFP-Rab21GTP–, or GFP-Rab21GDP–transfected HeLa cells (48 h) were lysed, and postnuclear supernatant was fractionated on a sucrose gradient and subjected to Western blot analysis with anti–α2-integrin and anti-GFP antibodies.

Published June 5, 2006

In these cells, internalized integrin did not colocalize with GFP-Rab11 (not depicted).

We also found that Rab5 and Rab21 regulated integrin internalization/recycling. The most rapid integrin internalization was observed in GFP-Rab5–expressing cells, in which 82–100% of the surface-labeled receptor internalized within 5 min (Fig. 3 B). GFP-Rab21 but not -Rab11 induced integrin internalization as well (74–86% after 10 min). Importantly, transferrin endocytosis was unaltered by Rab21 expression, suggesting that Rab21 does not influence the traffic of endosomally translocated receptors in general (Fig. S2 A, available at http://www.jcb.org/cgi/content/full/jcb.200509019/DC1). We are aware that we have not excluded the effects of Rab21 expression for all types of unspecific internalization (e.g., macropinocytosis), but at least its closest homologues (Rab5 and Rab22) have not been shown to affect macropinocytosis (Rosenfeld et al., 2001; Kauppi et al., 2002). Interestingly, the internalized receptor recycled rapidly back to the cell surface in Rab5- and Rab21-expressing cells with >50% of the labeled pool being recycled during a 15-min chase (detected by the reduction in the amount of biotinylated receptor in these cells where cell surface biotin is cleaved). Integrin internalization was reduced by expression of GFP-Rab21GDP, whereas GFP-Rab21GTP induced a steady accumulation of the internalized receptor when compared with GFP-, Rab5-, Rab11-, and Rab21GDP-expressing cells (Fig. 3 B, 30-min chase). Importantly, knock down of endogenous Rab21 reduced the amount of rapidly internalized integrin (Fig. 3 C, 5 min).

In density gradient fractionations, expression of GFP-Rab21 shifted the integrins toward the denser Rab-positive fractions (Hughes et al., 2002), and GFP-Rab21 cofractionated with α2-integrin in fractions 3–9 (Fig. 3 D). A further shift in the endogenous integrin pool (to fractions 5–11) was observed upon expression of GFP-Rab21GTP, and GFP-Rab21GDP was also observed in the denser fractions (Fig. 3 D). In the lighter fractions (3–5), GFP-Rab21 and integrin were found to cosediment with the Golgi-marker GM130, whereas in the denser fractions, cosedimentation was observed with the ER marker P115 (fractions 6–8) and EEA1 (fractions 7–9; Fig. S3 A, available at http://www.jcb.org/cgi/content/full/jcb.200509019/DC1). This data, together with the abundance of integrin vesicles observed

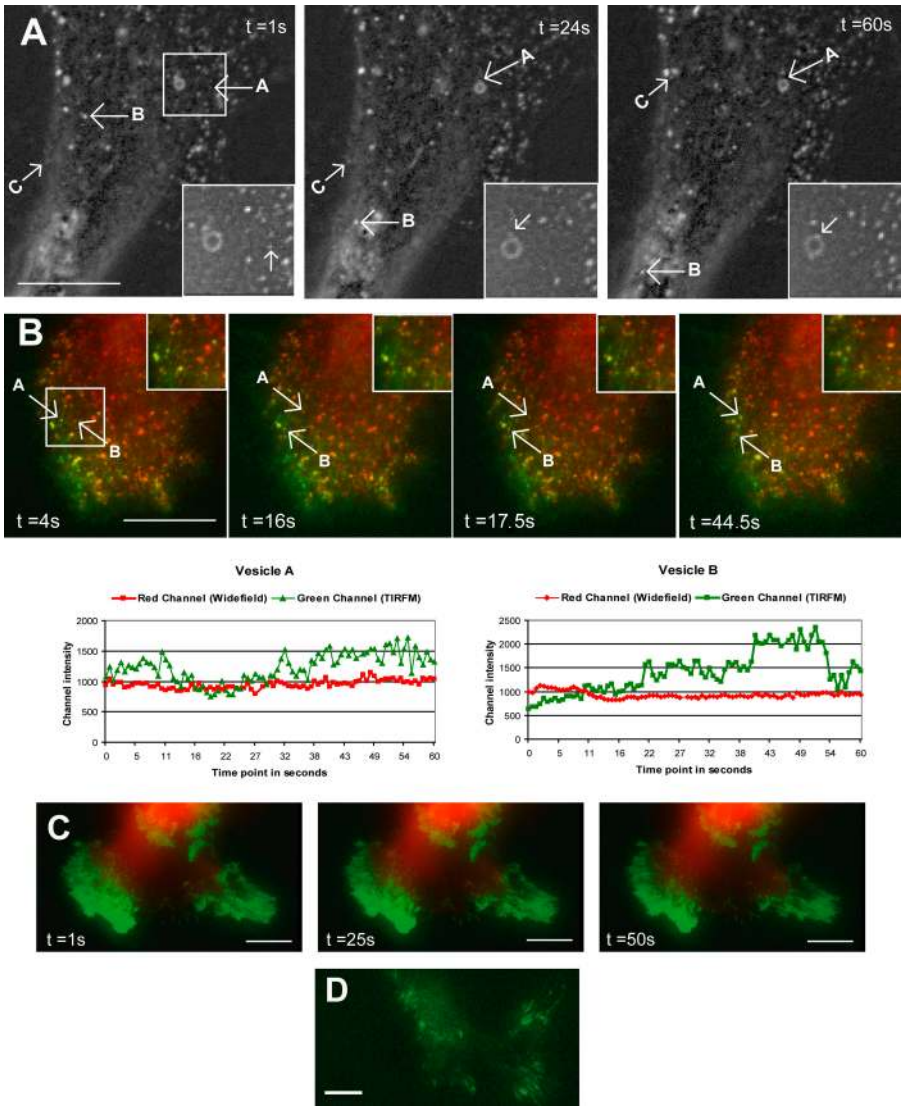

Figure 4. **GFP-Rab21 displays bidirectional movement between the plasma membrane and the cell body.** (A) Images of a time-lapse sequence displaying the bidirectional motility of GFP-Rab21–positive small vesicles (vesicles B and C) and their interaction with GFP-Rab21–positive large vesicles (vesicle A). Inset shows a higher magnification view of vesicle A. Bar, 5 μm. See Video 1 (available at http://www.jcb.org/cgi/content/full/jcb.200509019/DC1). (B and C) Combined widefield epifluorescence (pseudocolored red) and TIRFM (pseudocolored green) analysis of GFP-Rab21WT (B; see Video 2) or GFP-Rab21GDP (C; see Video 3) transfected cells. Images of time-lapse sequence displaying the mobility of GFP-Rab21–positive small vesicles between the cell membrane and the cell body. Times in seconds corresponding to each frame are indicated. Quantification plots (B) of two vesicles show fluorescence intensities detected by TIRFM (green) and widefield (red) for the same vesicles in each frame. (D) Representative still image from TIRFM (pseudocolored green) analysis of YFP-talin–transfected cells. Bars, 5 μm.

Published June 5, 2006

in Rab21-expressing cells (Fig. 2), suggests that Rab21 targets integrins to the endocytic fraction in human cells.

Further characterization of the large intracellular structures induced by GFP-Rab21 overexpression was performed by electron microscopy and immunogold labeling of GFP (Fig. S3, B and C). Overexpressed GFP-Rab21 was found predominantly on the limiting membranes of large multivesicular body (MVB)–like structures and in numerous vesicles surrounding it (Fig. S3, B and C), thus resembling the doughnut-shaped structures observed by immunofluorescence (Fig. 2). In addition, GFP-Rab21 staining was observed in structures with autophagic morphology (<20% of the labeled structures; unpublished data).

Rab21 expression induces motile GFP-integrin vesicles in live cells and displays bidirectional vesicle motility to and from the plasma membrane

We used time-lapse imaging to visualize the kinetics of Rab21 in real time. GFP-Rab21 was detected in large, swollen endosome-resembling structures, as well as in motile, smaller vesicles, which moved bidirectionally between the cytosol and the cell edges at velocity ranging from 0.75–2.25 μm/s (Fig. 4 A, vesicles B and C; and Video 1, available at http://www.jcb.org/cgi/content/full/jcb.200509019/DC1). Small vesicles were observed interacting with each other and associating with bright Rab21-containing domains on the larger Rab21-positive structures (Fig. 4 A, vesicle A) identical to the β1-integrin–containing vesicles seen in our immunofluorescence stainings (Figs. 1 and 2 and Fig. S1). The short-range motion of the Rab21 vesicles at the cell periphery was sensitive to the disruption of actin filaments with 20 μM cytochalasin (unpublished data), and the long-range curvilinear movements observed in the cell body were abolished upon treatment with 5 μM nocodazole (unpublished data), suggesting a role for actin and microtubules. Combined total internal reflection fluorescence microscopy (TIRFM; pseudocolored green) and conventional widefield epifluorescence analysis (pseudocolored red) showed GFP-Rab21 vesicles emanating from the membrane into the cell (changing from green to red/yellow) and back or vice versa (although formally this technique does not exclude the possibility that some vesicles will by chance come closer and further away from the plasma membrane). The intensity plots show rapid changes in the intensities of the signal in the green channel, whereas the signal in the red channel remains constant (Fig. 4 B and Video 2). No obvious diffusion of the bright Rab21 structures was seen using TIRFM, indicating either that the Rab21-labeled structures remain as distinct domains on the plasma membrane or that they do not fuse with the membrane. This former possibility correlates well with the observation that upon binding the small vesicles seem to remain as bright patches on the limiting membranes of the intracellular large Rab21-positive structures (Fig. 4 A). Real-time imaging and TIRFM confirmed that the intact GTP/GDP cycling of Rab21 was crucial for its vesicular traffic because motile small vesicles were not detected in GFP-Rab21GDP–transfected cells and Rab21 was associated with rather static structures at the cell membrane (Fig. 4 C and Video 3). These resemble YFP-talin–positive structures detected by TIRFM (Fig. 4 D) and may represent adhesion structures that have reduced turnover because of the expression of GFP-Rab21GDP and possibly its association with β1-integrin.

We also addressed whether Rab21 expression alters the motility of integrins in live cells. We engineered NH_2-terminally GFP-tagged α2-integrin (GFP-α2), which is dynamic in vivo, mediates cell adhesion to collagen, is recognized by α2I-domain binding monoclonal antibodies, and is expressed on the cell surface (see Fig. 6 E; not depicted). Upon cotransfection, Renilla luciferase (Rluc)–tagged Rab21 and GFP-α2 associated efficiently (Fig. 5 A). Rab21 expression induced motile GFP–α2-integrin–labeled vesicles (Fig. 5 B and Video 4, available at http://www.jcb.org/cgi/content/full/jcb.200509019/DC1),

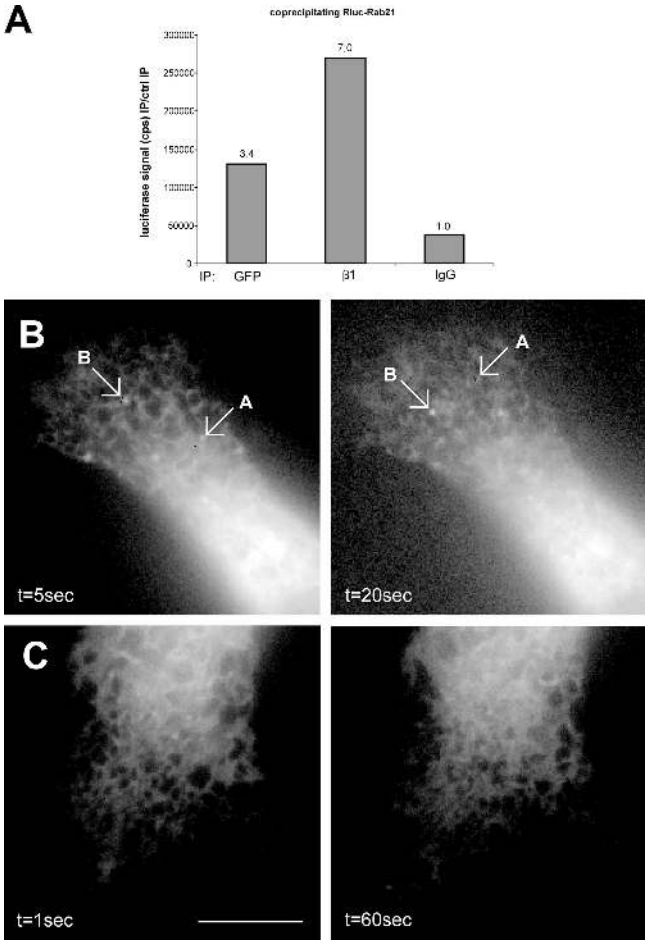

Figure 5. **Rab21 regulates the traffic of GFP–α2-integrin–positive vesicles.** (A) Cells transiently cotransfected with GFP-α2 and Rluc-Rab21 were subjected to the following immunoprecipitations (IPs): anti-GFP, anti-β1, and mouse IgG for control. The coprecipitated luciferase activity (cps) is shown, and the values above the bars indicate luminescence detected relative to the control immunoprecipitation. (B and C) MDA-MB-231 cells transfected with GFP–α2-integrin and Rluc-Rab21 (B) or with GFP–α2-integrin alone (C) were plated on collagen for 1 h, and time-lapse series were acquired with widefield epifluorescence microscopy. Cotransfected cells (B; see Video 4, available at http://www.jcb.org/cgi/content/full/jcb.200509019/DC1) show green fluorescent vesicles moving in the cytosol. No vesicles are visible in cells transfected with GFP–α2-integrin alone (C; see Video 5). Arrows labeled A and B point to two representative α2-integrin–positive vesicles. Bar, 5 μm.

Published June 5, 2006

whereas cells expressing GFP–α2-integrin alone or with Rluc-Rab21GDP, showed a vesicular-tubular staining pattern with no obvious vesicles and that partially overlaps with ER tracker stain in live cells (Fig. 5 C, Video 5, and not depicted). Collectively, these data demonstrate that enzymatically active Rab21 is able to target integrins to endocytic vesicles in live cells.

Rab21 regulates cell adhesion and migration of breast and prostate cancer cells

To investigate the importance of Rab21-mediated integrin traffic in β1-integrin–dependent cell adhesion, we studied MDA-MB-231 breast and PC3 prostate cancer cells having relatively high and low endogenous Rab21 expression, respectively (unpublished data). Of all the Rabs tested, overexpressed Rab21 was most efficient in increasing cell adhesion to collagen (86 ± 8% in PC3 cells and 22% in MDA-MB-231 cells; Fig. 6, A and B) during the initial 30 min of adhesion. Rab21 expression did not enhance the initial adhesion step of cells plated on fibronectin or vitronectin (Fig. S2 B). Expression of Rab5 increased adhesion by 48 ± 13% in PC3 cells. The GTP/GDP cycling of Rab21 was found to be important for supporting integrin function because the Rab21 mutants were unable to induce cell adhesion to collagen (Fig. 6 B). The lack of dominant effects of the mutants is probably due to the fact that their ectopic expression is not sufficient to interfere with the high number of endogenous associations between integrins and Rabs involved in regulating adhesion/migration, whereas introduction of Rab21WT supports adhesion to collagen by further increasing the endosomal traffic of α/β1-integrin heterodimers. Overexpression of GFP-Rab5, -Rab11, -Rab21, or -Rab21GTP did not influence the amount of β1-integrin detected on the surface of MDA-MB-231 (Fig. 6 C) and PC3 cells (not depicted), suggesting that efficient transport of endocytosed integrins to newly formed sites of adhesion, rather than a change in the steady-state expression of integrins on the cell surface, is the basis of Rab21-induced cell adhesion. Interestingly, GFP-Rab21GDP caused a modest increase in β1-integrin surface expression in MDA-MB-231 cells (Fig. 6 C). Thus, Rab21GDP both inhibits integrin traffic and increases cell surface levels of integrins. This induction of two counteracting forces further explains the lack of dominant-negative effects on adhesion. Most important, specific silencing of Rab21 with two different RNAi oligos (Fig. 6 D) resulted in a 30% reduction in the adhesion of MDA-MB-231 cells to collagen. As no down-regulation of β1-integrin was observed, the effect of Rab21 knockdown is most likely due to inefficient integrin traffic. Finally, to demonstrate that Rab21–integrin association is involved in Rab21-induced cell adhesion, we used the mutant α2-integrins with reduced Rab21 binding (Fig. 1, D and E). CHO cells lack endogenous collagen receptors. Transient expression of α2WT, α2AA (deficient Rab21 association), or α2A (unaltered Rab21 association), together with Rluc, enabled equivalent adhesion of these cells to collagen (Fig. 6 E, bottom). Rluc-Rab21 induced adhesion to collagen when coexpressed with α2WT- or α2A-integrins but failed to do so with α2AA-integrin mutant (Fig. 6 E, top). Furthermore, coexpression of Rluc-Rab21 induced vesicular localization of GFP-α2WT but had no effect on the cellular distribution of GFP-α2AA (Fig. 6 F).

The endo/exocytic cycle of integrins has been suggested to facilitate focal complex assembly as well as cell motility (Bretscher, 1996). We observed that the number of motile Rab21 vesicles close to the cell edge in the protruding lamellae was high in cells that were actively spreading on collagen or migrating at the edge of a scratch wound (Fig. 7 A, 1–2 h after plating; and not depicted) when compared with cells that had been adherent overnight or were located within a confluent monolayer (Fig. 7 A and not depicted). We also found that cells expressing GFP-Rab21WT migrated on plastic in a scratch wound assay to close the wound almost completely, whereas GFP-, GFP-Rab21GDP–, and GFP-Rab21GTP–expressing cells migrated less efficiently, covering only ∼70–75% of the wound area (Fig. 7 B). Conversely, stable Rab21-shRNA (short hairpin RNA)–transfected cells with reduced Rab21 expression (Fig. 3 C) migrated poorly, covering only ∼59% of the wound area, whereas Scr-shRNA–transfected control cells closed the wound almost completely (Fig. 7 C). During this time, there were no obvious differences in the proliferation of the stable transfected cells (not depicted). These data suggest that expression of Rab21 regulates migration in these cells.

Prostate and breast cancer cells are known to metastasize to bone (Mundy, 2002). Because fibrillar collagen is one of the main components in human bone, we finally analyzed the effects of Rab expression on cancer cell adhesion to bone matrix. Interestingly, overexpression of Rab21 in PC-3 prostate cancer cells resulted in a modest but constant and statistically significant (20 ± 8%; $n = 7$; $P < 0.03$) increase in adhesion to bone (Fig. 7 D). Together, our data show that Rab21 activity regulates integrin-dependent adhesion to collagen and human bone as well as the motility of cancer cells on cell-secreted and serum-derived matrix components other than collagen.

Discussion

We report the discovery of a previously unknown association between integrins and Rab proteins. We show that Rab5 and Rab21 associate with internalized integrins. Furthermore, Rab21 expression is shown to regulate integrin-containing focal adhesions and adhesion and migration of breast and prostate cancer cells. Live-cell imaging revealed that Rab21-positive vesicles move between the plasma membrane and the cell body and that expression of Rab21 modulates vesicular motility of integrins in vivo.

Although it is clear that the endocytic traffic of integrins involves a complex machinery of kinases, motor proteins, and members of the Rab family of GTPases, how integrins are actually targeted to the intracellular vesicles has remained enigmatic. The identification of integrin association with the putative early endosomal Rab21 led us to identify a functional relationship between integrin association with Rab21 and Rab5 and the regulation of cell adhesion. Several studies have demonstrated integrin endocytosis into intracellular vesicles and their recycling back to the membrane (Bretscher, 1989, 1992). In serum-starved cells stably adhering to tissue culture plastic, integrins have been

Published June 5, 2006

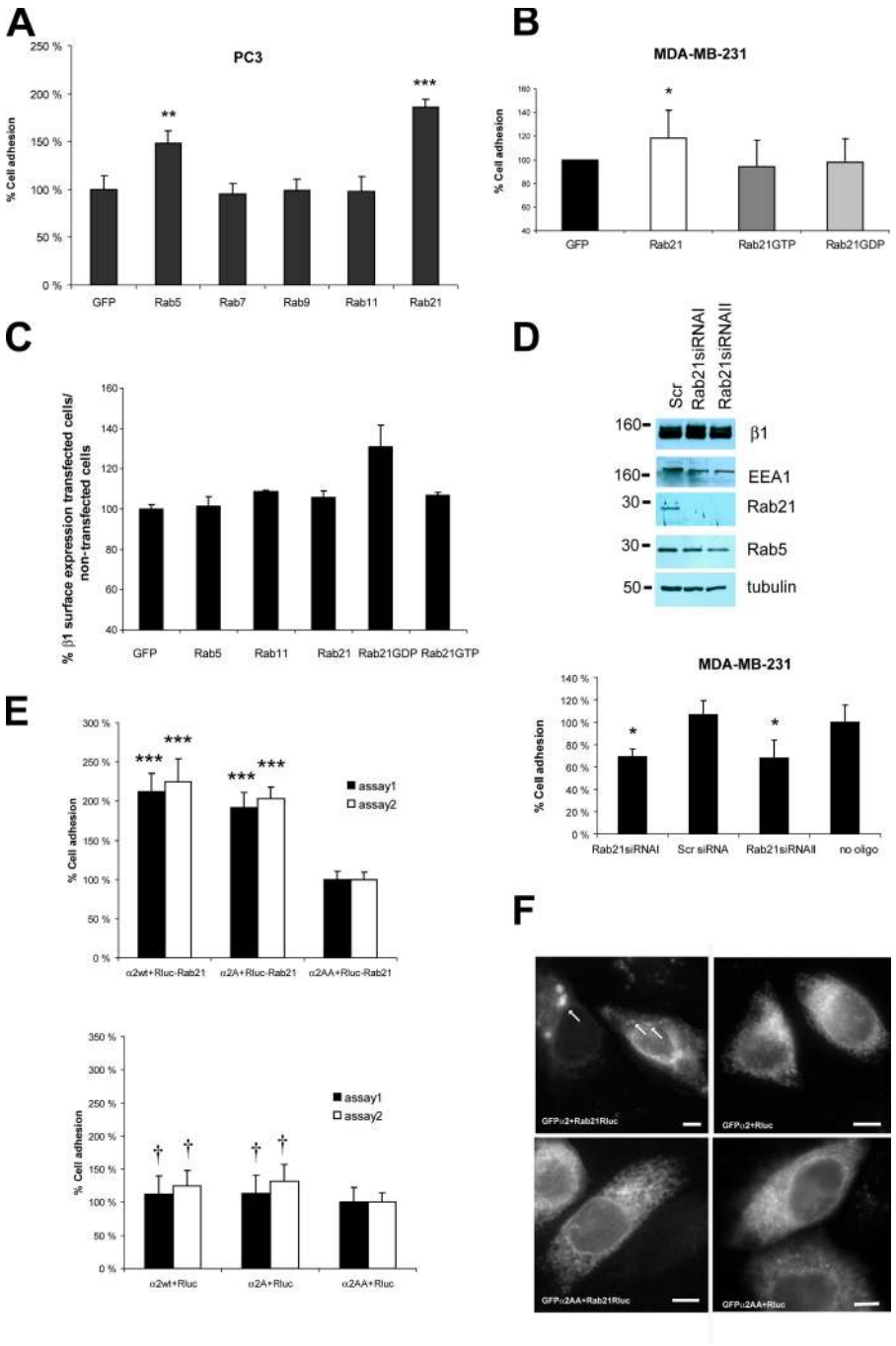

Figure 6. **Rab21 influences cell adhesion and migration.** (A and B) Adhesion of transiently transfected PC3 or MDA-MB-231 cells was studied on collagen (0.25 μg/ml CI, 30 min; means ± SD; $n = 12$; **, $P < 0.02$; ***, $P < 0.003$). (C) Cell surface expression of β1-integrin was analyzed with dual-color FACS from transiently transfected MDA-MB-231 cells. Mean fluorescence intensities (633-nm laser; β1-integrins) were detected from GFP-positive and -negative cells and are presented as a ratio (relative means ± SEM; $n = 4$). (D) MDA-MB-231 cells were transfected with two siRNAs specific for Rab21, scrambled control (Scr), or oligofectamine alone (no oligo). Adhesion to collagen and protein expression by immunoblotting were studied. A representative of three experiments with similar results is shown (mean ± SD; $n = 5$ parallel wells; *, $P < 0.02$). (E and F) CHO cells were transiently cotransfected with Rluc-Rab21 or Rluc and GFP-α2WT or mutants. (E) Adhesion was studied on collagen (105 min, two separate assays; means ± SEM; $n = 12$; ***, $P < 0.0001$; †, not significant). (F) Subcellular localization of GFP-integrin in the transfected collagen adhering cells was studied by widefield fluorescence microscopy. Arrows point to vesicular GFP-integrin. Bars, 4 μm.

shown to be transported to a perinuclear recycling compartment. Upon growth factor stimulus, internalized integrins either recycle very rapidly back to the plasma membrane from the perinuclear compartment (β1-integrins; Powelka et al., 2004) or are completely rerouted to a short-loop trafficking pathway directly back to the membrane (αvβ3-integrin; Roberts et al., 2004). The existence of a Rab–integrin association, which positively regulates cell adhesion, provides a missing mechanistic link into the orchestration of this complex process. We show on one hand that the motility of Rab21 vesicles close to the plasma membrane requires the actin cytoskeleton and, on the other hand, that expression of Rab21 mutants with impaired GTP binding or membrane localization induce integrin targeting to the membrane and the formation of exaggerated adhesion sites. This is in agreement with the recent finding that integrins in newly forming protrusions travel on actin cables associated to motor protein Myosin X and that normal cell adhesion and spreading during the initial stages of adhesion seem to require the efficient motility of integrins close to the plasma membrane (Zhang et al., 2004).

There is only limited data available on the dynamics of integrins in cells. One study demonstrates the internalization of GFP-tagged integrin in live cells (Laukaitis et al., 2001). However, no integrin movements back to the plasma membrane were seen. Although the role of Rab proteins was not addressed in the

Published June 5, 2006

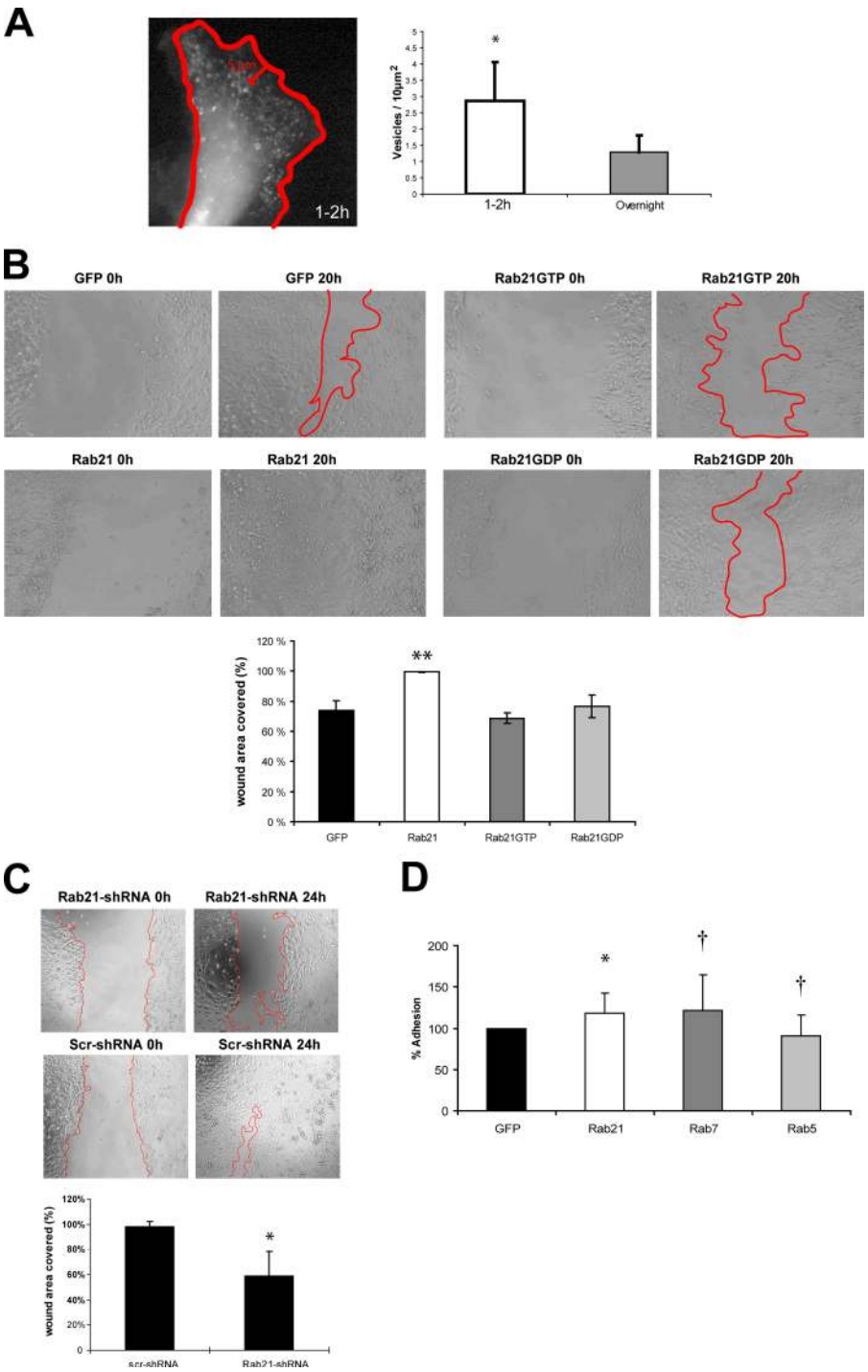

Figure 7. **Rab21 influences cell migration.** (A) GFP-Rab21 transfected MDA-MB-231 cells on collagen (time-lapse series 60 s each) were imaged. Number of vesicles per area near the edges (5 µm; mean ± SD; *, $P < 0.05$) were quantified at two time points after plating (1–2 h, 9 cells; overnight, 6 cells). (B and C) Migration of MDA-MB-231 cells stably expressing GFP, GFP-Rab21, GFP-Rab21GTP, GFP-Rab21GDP, Rab21-shRNA, or Scr-shRNA was studied using the scratch wound assay (migration 24 h in 10% FBS). Analyses of wound areas covered by the cells are shown (means ± SD; $n = 4$–7; *, $P < 0.01$; **, $P < 0.001$). (D) Adhesion of transfected PC3 cells to bone (Cambrex OsteoAssay plate; mean ± SD; $n = 7$; *, $P < 0.03$; †, not significant).

study of Laukaitis et al. (2001), it is intriguing to note that the large vesicles they described are remarkably similar to the structures induced here by the overexpression of GFP-Rab21. We show here that these large structures resemble MVBs. MVBs are generally thought of as being major protein sorting stations in the endocytic pathway. Proteins at their limiting membrane can be packaged into transport vesicles destined to the cell surface or to the TGN. Alternatively, proteins can be targeted to inwardly budding vesicles of the MVBs. These latter are considered to be the exosomes secreted after fusion of MVBs with the plasma membrane (Fevrier and Raposo, 2004). The observation that overexpressed GFP-Rab21 is seen mainly in the limiting membrane and vesicles surrounding the MVBs points to an involvement of the MVBs in recycling vesicles back to the plasma membrane. The enlargement of the MVBs and accumulation of the vesicles most likely is the result of overexpression of the Rab21 protein, indicating its role in traffic to the MVBs. Our data does not unambiguously show whether integrins and Rabs interact directly. The facts that the association was detected from a yeast two-hybrid screen and that it is abrogated by mutagenesis

Published June 5, 2006

of the α-cytoplasmic domain suggest that it may be direct. However, we cannot rule out the possibility that as-yet-unknown proteins that are capable of binding to the integrin may serve as linkers between Rab21 and integrins. We were unable to detect direct interaction of GST-Rab21 with synthetic integrin cytoplasmic tail peptides. However, this does not necessarily mean that the interaction is not direct. It is possible that the peptides are not presented in a correct conformation for the interaction to occur. Evidence from detailed biochemical and nuclear magnetic resonance studies (Stefansson et al., 2004; Vinogradova et al., 2004) indicates that upon integrin activation the membrane-proximal regions of the integrin cytoplasmic tails move out of the membrane into the cytoplasm, revealing the highly conserved residues to the cytoplasmic face and involving substantial structural changes in the cytoplasmic tails. We show that Rab21–integrin association occurs downstream of the internalization step and that a substantial portion of the internalized integrin is in an active conformation as detected by the activation epitope–specific antibodies. This is in line with our data showing that the association is mediated via the membrane proximal–conserved segment of the α-subunit COOH terminus, with conserved residue R1161 being especially important, and that the association seems to be α-tail conformation sensitive.

Prenylation-dependent membrane targeting of Rabs is crucial for Rab function as regulators of vesicle fusion in intracellular protein trafficking (Desnoyers et al., 1996). We show that the mutagenesis of the putative prenylation motif in Rab21 results in complete loss of its vesicular localization. At the same time, this variant shows reduced association with β1-integrins and upon overexpression induces integrin localization on the plasma membrane and in large focal adhesions (by targeting the integrins or by blocking the internalization).

Rab21 and integrin internalization routes

Endocytosis encompasses several routes of internalization. The entry route of integrins remains somewhat unclear and may vary between different heterodimers. Integrins have been shown to internalize in a dynamin and PKCα-dependent manner after ligand binding (Ng et al., 1999). Internalized β1-integrins are then targeted to caveosomes (Upla et al., 2004) or transferrin-positive endosomes (Laukaitis et al., 2001) depending on the heterodimer, the cell type, and the stimulus used. Recent data showing that the caveolar and endosomal pathways intersect (Pelkmans et al., 2004) and our data showing caveolin-1–positive domains on Rab5- and Rab21-positive integrin–containing vesicles provide a possible explanation for these variable integrin trafficking routes. We show that several different integrin heterodimers associate with Rab21. This association may serve to target integrins that initially enter the cell via different routes to the same trafficking pathway.

From the live-cell TIRFM studies, it is obvious that Rab21-positive structures traffic from the cell body to the plasma membrane, possibly delivering integrins to adhesion sites. This correlates well with the previous work showing that α5-integrin engagement initiates the newly forming adhesions and serves to organize proteins like paxillin in these sites (Laukaitis et al., 2001).

We show here that Rab21 expression induces cell motility and adhesion to collagen and to human bone in vitro. Importantly, Rab21 is also able to induce the endosomal traffic of integrins. Interestingly, emerging evidence implicates alterations in the Rab small GTPases and their associated regulatory proteins and effectors in multiple human diseases, including cancer (Cheng et al., 2004). In conclusion, the identification of Rab21–integrin association opens new opportunities for investigating the detailed mechanisms underlying the adhesion and migration of cells in vivo in diseases like cancer metastasis.

Materials and methods

Antibodies and DNA constructs

Antibodies against the following antigens were used: EEA1, Rab5A, Rab7, Rab11, caveolin-1 (all from Santa Cruz Biotechnology, Inc.), Rab21 (Opdam et al., 2000), β1-integrin (P5D2, P4G11, and AIIB2), α5-integrin (BIIG2), EGFR (151-IgG; all from the Drosophila Studies Hybridoma Bank), α2 (mAb MCA2025; Serotec), pAb AB1934 (Chemicon), α1 (MAB1973; Chemicon), α6 (MAB699; Chemicon), β1 (HUTS-21 [BD Biosciences] and MAB2252 [Chemicon]), collagen type 1 (RAHC11; Imtek), GFP polyclonal antibody, fluorescently conjugated secondary antibodies, Cell Tracker dyes, and labeled transferrin (all from Invitrogen).

Full-length Rab21 was subcloned from Rab21 murine cDNA (clone 6490069; IMAGE) by PCR amplification and ligated into pRluc-C2 (PerkinElmer) and in pEGFP-C2 (CLONTECH Laboratories, Inc.). Rab21GTP (Q76L), Rab21GDP (T31N), and CCSS (residues 218 and 219) mutants were generated using QuikChange Site-directed mutagenesis kit (Stratagene). Rab21 COOH-terminal–deletion mutant was generated by introducing a stop codon after E144. Plasmids encoding GFP-Rab5a, GFP-Rab7, YFP-Rab9, and GFP-Rab11 have been described (Wilcke et al., 2000; Barbero et al., 2002; Lebrand et al., 2002; Gomes et al., 2003), and YFP-mouse talin was provided by D. Critchley (University of Leicester, Leicester, UK). α2-Integrin was subcloned from the α2 cDNA in pawneo2 vector (Ivaska et al., 1999) into pEGFP-C2 vector. The signal sequence of α2-integrin (annealed synthetic oligos corresponding to nucleotides 43–129 in the published sequence [Takada and Hemler, 1989] was inserted to the NheI site in the vector to enable correct targeting to the plasma membrane. The GFP–α2-integrin cytoplasmic tail mutants were generated by using QuikChange Site-directed mutagenesis kit. All clones were verified by sequencing.

Immunoprecipitations

Rluc-tagged Rab21 constructs alone or with GFP-α2 variants (CHO cells that lack endogenous collagen binding integrins) were transfected into 95% confluent cells using Lipofectamine 2000 and incubated for 18 h. For immunoprecipitations with endogenous proteins, confluent MDA-MB-231 cells (20×10^6) were collected from plastic plates with cold PBS. For analysis of association with cell surface–labeled integrin, MDA-MB-231 cells were plated on collagen-coated dishes for 1 h and surface biotinylated with cleavable biotin (0.5 mg/ml EZ-sulfo-NHS-SS-biotin in HANKS buffer) for 30 min on ice. After washings, cells were either lysed immediately or warmed for 15 min in HANKS +37°C to allow internalization. Cells were lysed in IP buffer (PBS with 1% octylglycoside, 0.5% BSA, 1mM $CaCl_2$, 1mM $MgCl_2$, and protease inhibitor cocktail [Roche]) on ice for 15 min. Postcentrifugation supernatant was precleared with BSA-blocked (IP buffer) protein G–agarose beads and divided into five aliquots for immunoprecipitations with different anti-Rab antibodies or a control antibody and protein G beads (90-min rotation at 4°C). After three washings (IP buffer containing 0.3% octylglycoside), SDS sample buffer was added and the proteins were separated by SDS-PAGE (4%/10%) and immunoblotted for β1-integrin (MAB2252). Reimmunoprecipitations were performed as described earlier (Mattila et al., 2005). For the luminescent immunoprecipitations, the beads were transferred into white microtiter plate wells (96-well) and treated with Rluc substrate (5 μg/ml coelenterazine [Nanolight Technologies]), and the luminescence was measured with a multilabel HTS counter (Victor^{2}V; PerkinElmer).

Integrin internalization and recycling assay

These were performed as described previously (Roberts et al., 2001; Ivaska et al., 2002) with some modifications. After 1 h of adhesion to

Published June 5, 2006

collagen-coated dishes, the transfected cells were placed on ice, washed once with cold PBS, and surface labeled with 0.5 mg/ml cleavable NHS-SS-biotin (Pierce Chemical Co.). After washings, prewarmed (+37°C) HANKS medium was added, and protein traffic (internalization and recycling) was allowed to occur for the times indicated. Biotin was removed from cell surface proteins by MesNa reduction and iodoacetamide quenching on ice. The cells were lysed (200 mM NaCl, 75 mM Tris, 15 mM NaF, 1.5 mM Na_3VO_4, 7.5 mM EDTA, 7.5 mM EGTA, 1.5% Triton-X-100, and Complete), and the amount of biotinylated integrin was assayed using the anti–β1-integrin antibody AIIB2 to capture the integrins and HRP anti-biotin antibody for ELISA detection. As control, the cells were lysed after the labeling to determine the amount of total biotinylated integrin.

Immunoelectron microscopy

Stable MDA-MB-231–expressing GFP-Rab21 cells were fixed in 1% PFA with or without 0.01% glutaraldehyde in 100 mM phosphate buffer, pH 7.0, for 2 h at RT. Next, cells were pelleted in 10% gelatine and postfixed in 1% PFA for another 24 h. Ultrathin cruosections were prepared on a cryochamber (EM FCS; Leica), and thawed sections were incubated with a polyclonal antiserum raised against EGFP followed by incubation with protein A complexed to 5-nm gold particles according to standard procedures. Sections were observed in an electron microscope (model 1010; JEOL) operating at 80 kV.

Sucrose gradient fractionations

HeLa cells were transiently transfected with GFP, GFP-Rab21, or GFP-Rab21GTP using Lipofectamine 2000 as described in the Immunoprecipitations section. 48 h after transfection, the cells were harvested and fractionated on a sucrose density gradient and analyzed by Western blotting as described previously (Hughes et al., 2002).

Yeast two-hybrid screen and yeast mating tests

The α2-integrin COOH-terminal tail (28 residues) Gal4 DNA binding domain fusion (pGBKT7 vector) was used to screen a mouse E17 Matchmaker cDNA library (CLONTECH Laboratories, Inc.) as described previously (Mattila et al., 2005). In yeast mating tests, pGADT7-Rab21 (95–222) prey was transformed in Y187 host strain and cytoplasmic tails of α2- and α11-integrin (pGBKT7-α2 and -α11) and their variants in AH109 host strain. Point mutants were generated with the QuikChange Site-directed mutagenesis kit and confirmed by sequencing. The negative and positive controls in yeast mating tests were pGBKT7-53/pGADT7-T and pGBKT7/pGADT7, respectively.

Cell lines and RNAi transfections

MDA-MB-231 cells (American Type Culture Collection) were grown in DME + 1% nonessential amino acids and 10% FBS. Saos-2, HeLa, HT1080, and HEK293T cells (American Type Culture Collection) were grown in DME + 10% FBS, and PC3 cells (American Type Culture Collection) were grown in F12 medium + 10% FBS. CHO cells (American Type Culture Collection) were grown in MEM Alpha Medium + 5% FBS. Saos-2 cells express no endogenous α2 (Ivaska et al., 1999). Stable Saos-2 cells expressing equal levels of chimeric integrins (extracellular domain of α2 fused with α1 or α5 cytoplasmic tails; Ivaska et al., 1999) have been described (Mattila et al., 2005). Two different annealed siRNAs targeting Rab21 (sense, ggcaucauucuuaacaaagtt and ggucaagagagauuccaugtt; Ambion) or scramble control siRNA (Silencer Negative control #1 siRNA; Ambion) were transfected at a 100-nM concentration to MDA-MB-231 or PC3 cells using Oligofectamine (Invitrogen) according to the manufacturer's protocol (48-h culture). pSilencer 4.1-CMV hygro vector (Ambion) was used to express shRNAs. Annealed DNA oligos (Scr sense strand, gatccgcgaatcctacaagcgcgcttgatatccggcgcgctttgtaggattcgtttttccaaa; Rab21 sense strand, gatccggtcaagagagagettccatgttcaagagacatggaatctctcttgacctga) were ligated to the vector between BamHI and HindIII sites. Plasmids were verified by sequencing. shRNA plasmids and transfected into MDA-MB-231 cells using Lipofectamine 2000 (Invitrogen), and stable cell clones were generated with hygromycin selection.

Adhesion and migration assays

96-well plates were coated with collagen or fibronectin (0.25 μg/ml) overnight and blocked with 0.1% BSA (1 h, 37°C). Transiently transfected cells (GFP-Rabs or siRNA) were harvested, trypsin inhibited with 0.2% (wt/vol) Soybean trypsin inhibitor, and stained (only siRNA-transfected cells) with CellTracker Green CMFDA (Invitrogen) according to the manufacturer's instructions. Cells were suspended in 0.5% BSA in serum-free DME, seeded (5,000 cells/well) on the plates, and allowed to adhere for 30 min at 37°C. After one washing with PBS, cells were fixed (4% PFA, 10 min). Adhesion was measured by counting the number of green fluorescent cells using Acumen Assay Explorer 488 nm. The total number of GFP-positive cells was assayed after adhesion to collagen for 4 h in the presence of 10% FBS. Adhesion assays with CHO cells were done by cotransfecting GFP-α2WT or GFP-α2CYTOKR1160/61AA mutant together with Rluc-Rab21 or Rluc alone. The assays were done as described earlier in this paragraph, except that the specific adhesion time on collagen was lengthened to 1 h and 45 min.

For the scratch wound assay, stable MDA-MB-231 cells expressing GFP, GFP-Rab21, GFP-Rab21GTP, or GFP-Rab21GDP were generated. The cells were seeded onto collagen-coated 96-well plates at 35,000 cells/well and allowed to adhere overnight in the presence of 10% FBS. The wound was generated by scratching with a plastic tip. Images were taken from each well immediately and after 20 h, and the wound areas were analyzed using AxioVision 4.3 software (Carl Zeiss MicroImaging, Inc.). The number of live cells (proliferation) was scored at 0 and 20 h from identical wells using WST-1 (Roche).

For the human bone adhesion assay, transfected PC3 cells were resuspended in serum-free DME, seeded 10,000 cells/well (Cambrex OsteoAssay plate [PA-1000]), and allowed to adhere for 45 min before fixation as described earlier in this section. Green fluorescent cells were counted using a widefield epifluorescence microscope (narrow GFP filter and 20× objective). The total number of transfected cells was assayed as described earlier in this section.

Immunofluorescence

Cells were plated on acid-washed glass coverslips coated with 5 μg/ml collagen type I, allowed to adhere for 1 h, washed in PBS, and PFA fixed. After permeabilization (PBS/0.02% saponin/10% FBS, 15 min), cells were stained with primary antibodies (in the same buffer) for 1 h at RT. After three washings, Alexa 488–, Alexa 555–, or Alexa 647–conjugated secondary antibodies were added (in the same buffer). Slides were examined using an inverted fluorescence microscope (Carl Zeiss MicroImaging, Inc.) or a confocal laser-scanning microscope (Axioplan 2 with LSM 510; Carl Zeiss MicroImaging, Inc.) equipped with 100×/1.4 Plan-Apochromat oil-immersion objectives. Confocal images represent a single z section of ∼1.0 μm. β1-Integrin and transferrin internalization were studied as described previously (Powelka et al., 2004).

Live-cell microscopy

A multilaser microscope (IX81; Olympus) equipped with a 488-nm TIRF condensor and a 60×/1.4 Plan-Apochromat oil-immersion objective was used for TIRFM. TIRFM was combined with conventional widefield epifluorescence microscopy and time-lapse series (frame rate ∼2/s) Widefield images were pseudocolored red and TIRFM images green. Transiently transfected GFP-Rab21 cells were plated on acid-washed glass-bottomed dishes (MatTek Corporation) coated with 10 μg/ml collagen type I and allowed to adhere for 1 h before microscopy. Clear medium with 2.2 g/l NaHCO3 was used for imaging in heat (37°C) and CO_2 (5%) stable environment box.

The Axioplan 2 microscope equipped with Plan-Apochromat 63× (NA 1.4) objective and a camera (Orca 2; Hamamatsu Photonics) was used for widefield epifluorescence time-lapse imaging at a rate of 2 frames/s. GFP-Rab21 and its mutant variants (or Rluc-Rab21 and GFP–α2-integrin in the cotransfection studies) were transfected to MDA-MB-231 adenocarcinoma cells. Clear DME 4500 supplemented with 1% L-glutamine, 0.5% BSA, and 30 mM Hepes was used as imaging medium. Microscopy was performed in a heat-stable environment for no longer than 1 h. MetaMorph imaging software (Universal Imaging Corp.) was used in image analysis.

Statistical analysis

Fluorescence intensities for TIRFM and widefield epifluorescence microscopy were measured and analyzed with MetaMorph software. Vesicle intensities from time-lapse series were background corrected in each time point with the formula $(I_B - I_V) \times (A_V/[A_B - A_V])$, where I is integrated intensity for region area A. B stands for background and V for vesicle. Region for vesicle (A_V) was created just around vesicle and region for background (A_B) just around the vesicle region. Results from two groups were compared using a *t* test, and statistical significance was set at $P < 0.05$.

Online supplemental material

Fig. S1 shows the cellular localization of endogenous β1-integrin, caveolin-1, Rab21, and EEA1 in MDA-MB-231 cells expressing GFP-Rab5 or -Rab21 and internalization of β1-integrin antibody and labeled transferrin

in GFP-Rab5– and GFP-Rab21–expressing cells. Fig. S2 shows that overexpression of Rab21 does not influence the traffic of labeled transferrin in cells or the adhesion of cells to matrixes other than type I collagen. Fig. S3 shows the localization of organelle markers on the sucrose gradient–fractionated GFP-Rab21–expressing HeLa cells and immunogold electron micrographs of GFP-Rab21–positive structures in MDA-MB-231 cells. Table S1 demonstrates the association of Rab21WT and its variants with α/β1-integrin heterodimers in HT1080 cells. Video 1 shows MDA-MB-231 cells expressing GFP-Rab21, adhering to collagen recorded on GFP channel. Video 2 shows a combined widefield epifluorescence and TIRFM analysis of MDA-MB-231 cells expressing GFP-Rab21, adhering to collagen. Video 3 shows a combined widefield epifluorescence and TIRFM analysis of MDA-MB-231 cells expressing GFP-Rab21GDP mutant, adhering to collagen. Video 4 shows MDA-MB-231 cells cotransfected with GFP–α2-integrin and Rluc-Rab21WT, adhering to collagen recorded on GFP channel. Video 5 shows MDA-MB-231 cells transfected with GFP–α2-integrin alone adhering to collagen recorded on GFP channel. Online supplemental material is available at http://www.jcb.org/cgi/content/full/jcb.200509019/DC1.

We acknowledge R. Pepperkok and J. Rietdorf in the Advanced Light Microscopy Facility at the European Molecular Biology Laboratory for help with the TIRFM studies and M. Kallio for help with the vesicle quantitations. We thank M. Salmi and M. Way for critically reviewing the manuscript; Drs. M.C. Seabra, S. Pfeffer, and B. Goud for plasmids; and H. Jalonen and M. Wiejers for their excellent technical assistance.

This work was supported by grants from the Academy of Finland, the Sigrid Juselius Foundation, Emil Aaltonen Foundation, and Finnish Cancer Organizations.

Submitted: 6 September 2005
Accepted: 8 May 2006

References

Barbero, P., L. Bittova, and S.R. Pfeffer. 2002. Visualization of Rab9-mediated vesicle transport from endosomes to the trans-Golgi in living cells. *J. Cell Biol.* 156:511–518.

Bretscher, M.S. 1989. Endocytosis and recycling of the fibronectin receptor in CHO cells. *EMBO J.* 8:1341–1348.

Bretscher, M.S. 1992. Circulating integrins; alpha 5, beta 1, alpha 6 beta 4 and Mac-1, but not alpha 3 beta 1, alpha 4 beta 1 or LFA-1. *EMBO J.* 11:405–410.

Bretscher, M.S. 1996. Moving membrane up to the front of migrating cells. *Cell.* 85:465–467.

Caswell, P.T., and J.C. Norman. 2006. Integrin trafficking and the control of cell migration. *Traffic.* 7:14–21.

Cheng, K.W., J.P. Lahad, W.L. Kuo, A. Lapuk, K. Yamada, N. Auersperg, J. Liu, K. Smith-McCune, K.H. Lu, D. Fishman, et al. 2004. The RAB25 small GTPase determines aggressiveness of ovarian and breast cancers. *Nat. Med.* 10:1251–1256.

Desnoyers, L., J.S. Anant, and M.C. Seabra. 1996. Geranylgeranylation of Rab proteins. *Biochem. Soc. Trans.* 24:699–703.

Fevrier, B., and G. Raposo. 2004. Exosomes: endosomal-derived vesicles shipping extracellular messages. *Curr. Opin. Cell Biol.* 16:415–421.

Gomes, A.Q., B.R. Ali, J.S. Ramalho, R.F. Godfrey, D.C. Barral, A.N. Hume, and M.C. Seabra. 2003. Membrane targeting of Rab GTPases is influenced by the prenylation motif. *Mol. Biol. Cell.* 14:1882–1899.

Hughes, W.E., B. Larijani, and P.J. Parker. 2002. Detecting protein-phospholipid interactions. Epidermal growth factor-induced activation of phospholipase D1b in situ. *J. Biol. Chem.* 277:22974–22979.

Huttenlocher, A. 2005. Cell polarization mechanisms during directed cell migration. *Nat. Cell Biol.* 7:336–337.

Hynes, R.O. 2002. Integrins: bidirectional, allosteric signaling machines. *Cell.* 110:673–687.

Ivaska, J., H. Reunanen, J. Westermarck, L. Koivisto, V.M. Kahari, and J. Heino. 1999. Integrin α2β1 mediates isoform-specific activation of p38 and upregulation of collagen gene transcription by a mechanism involving the α2 cytoplasmic tail. *J. Cell Biol.* 147:401–416.

Ivaska, J., R.D. Whelan, R. Watson, and P.J. Parker. 2002. PKC epsilon controls the traffic of beta1 integrins in motile cells. *EMBO J.* 21:3608–3619.

Kauppi, M., A. Simonsen, B. Bremnes, A. Vieira, J. Callaghan, H. Stenmark, and V.M. Olkkonen. 2002. The small GTPase Rab22 interacts with EEA1 and controls endosomal membrane trafficking. *J. Cell Sci.* 115:899–911.

Laukaitis, C.M., D.J. Webb, K. Donais, and A.F. Horwitz. 2001. Differential dynamics of α5 integrin, paxillin, and α-actinin during formation and disassembly of adhesions in migrating cells. *J. Cell Biol.* 153:1427–1440.

Lebrand, C., M. Corti, H. Goodson, P. Cosson, V. Cavalli, N. Mayran, J. Faure, and J. Gruenberg. 2002. Late endosome motility depends on lipids via the small GTPase Rab7. *EMBO J.* 21:1289–1300.

Lenter, M., H. Uhlig, A. Hamann, P. Jeno, B. Imhof, and D. Vestweber. 1993. A monoclonal antibody against an activation epitope on mouse integrin chain beta 1 blocks adhesion of lymphocytes to the endothelial integrin alpha 6 beta 1. *Proc. Natl. Acad. Sci. USA.* 90:9051–9055.

Luque, A., M. Gomez, W. Puzon, Y. Takada, F. Sanchez-Madrid, and C. Cabanas. 1996. Activated conformations of very late activation integrins detected by a group of antibodies (HUTS) specific for a novel regulatory region (355-425) of the common beta 1 chain. *J. Biol. Chem.* 271:11067–11075.

Mattila, E., T. Pellinen, J. Nevo, K. Vuoriluoto, A. Arjonen, and J. Ivaska. 2005. Negative regulation of EGFR signalling through integrin-alpha1beta1-mediated activation of protein tyrosine phosphatase TCPTP. *Nat. Cell Biol.* 7:78–85.

Miaczynska, M., and M. Zerial. 2002. Mosaic organization of the endocytic pathway. *Exp. Cell Res.* 272:8–14.

Mould, A.P., A.N. Garratt, J.A. Askari, S.K. Akiyama, and M.J. Humphries. 1995. Identification of a novel anti-integrin monoclonal antibody that recognises a ligand-induced binding site epitope on the beta 1 subunit. *FEBS Lett.* 363:118–122.

Mundy, G.R. 2002. Metastasis to bone: causes, consequences and therapeutic opportunities. *Nat. Rev. Cancer.* 2:584–593.

Naslavsky, N., R. Weigert, and J.G. Donaldson. 2003. Convergence of non-clathrin- and clathrin-derived endosomes involves Arf6 inactivation and changes in phosphoinositides. *Mol. Biol. Cell.* 14:417–431.

Ng, T., D. Shima, A. Squire, P.I. Bastiaens, S. Gschmeissner, M.J. Humphries, and P.J. Parker. 1999. PKCalpha regulates beta1 integrin-dependent cell motility through association and control of integrin traffic. *EMBO J.* 18:3909–3923.

Opdam, F.J., G. Kamps, H. Croes, H. van Bokhoven, L.A. Ginsel, and J.A. Fransen. 2000. Expression of Rab small GTPases in epithelial Caco-2 cells: Rab21 is an apically located GTP-binding protein in polarised intestinal epithelial cells. *Eur. J. Cell Biol.* 79:308–316.

Pelkmans, L., T. Burli, M. Zerial, and A. Helenius. 2004. Caveolin-stabilized membrane domains as multifunctional transport and sorting devices in endocytic membrane traffic. *Cell.* 118:767–780.

Powelka, A.M., J. Sun, J. Li, M. Gao, L.M. Shaw, A. Sonnenberg, and V.W. Hsu. 2004. Stimulation-dependent recycling of integrin beta1 regulated by ARF6 and Rab11. *Traffic.* 5:20–36.

Roberts, M., S. Barry, A. Woods, P. van der Sluijs, and J. Norman. 2001. PDGF-regulated rab4-dependent recycling of alphavbeta3 integrin from early endosomes is necessary for cell adhesion and spreading. *Curr. Biol.* 11:1392–1402.

Roberts, M.S., A.J. Woods, P.E. Shaw, and J.C. Norman. 2003. ERK1 associates with alpha(v)beta 3 integrin and regulates cell spreading on vitronectin. *J. Biol. Chem.* 278:1975–1985.

Roberts, M.S., A.J. Woods, T.C. Dale, P. Van Der Sluijs, and J.C. Norman. 2004. Protein kinase B/Akt acts via glycogen synthase kinase 3 to regulate recycling of alpha v beta 3 and alpha 5 beta 1 integrins. *Mol. Cell. Biol.* 24:1505–1515.

Rosenfeld, J.L., R.H. Moore, K.P. Zimmer, E. Alpizar-Foster, W. Dai, M.N. Zarka, and B.J. Knoll. 2001. Lysosome proteins are redistributed during expression of a GTP-hydrolysis-defective rab5a. *J. Cell Sci.* 114:4499–4508.

Seachrist, J.L., S.A. Laporte, L.B. Dale, A.V. Babwah, M.G. Caron, P.H. Anborgh, and S.S. Ferguson. 2002. Rab5 association with the angiotensin II type 1A receptor promotes Rab5 GTP binding and vesicular fusion. *J. Biol. Chem.* 277:679–685.

Simpson, J.C., G. Griffiths, M. Wessling-Resnick, J.A. Fransen, H. Bennett, and A.T. Jones. 2004. A role for the small GTPase Rab21 in the early endocytic pathway. *J. Cell Sci.* 117:6297–6311.

Stefansson, A., A. Armulik, I. Nilsson, G. von Heijne, and S. Johansson. 2004. Determination of N- and C-terminal borders of the transmembrane domain of integrin subunits. *J. Biol. Chem.* 279:21200–21205.

Takada, Y., and M.E. Hemler. 1989. The primary structure of the VLA-2/collagen receptor α2 subunit (platelet GPIa): homology to other integrins and the presence of a possible collagen-binding domain. *J. Cell Biol.* 109:397–407.

Upla, P., V. Marjomaki, P. Kankaanpaa, J. Ivaska, T. Hyypia, F.G. Van Der Goot, and J. Heino. 2004. Clustering induces a lateral redistribution of alpha 2 beta 1 integrin from membrane rafts to caveolae and subsequent protein kinase C-dependent internalization. *Mol. Biol. Cell.* 15:625–636.

van IJzendoorn, S.C.D., M.J. Tuvim, T. Weimbs, B.F. Dickey, and K.E. Mostov. 2002. Direct interaction between Rab3b and the polymeric immunoglobulin

Published June 5, 2006

receptor controls ligand-stimulated transcytosis in epithelial cells. *Dev Cell.* 2:219–228.

Vinogradova, O., J. Vaynberg, X. Kong, T.A. Haas, E.F. Plow, and J. Qin. 2004. Membrane-mediated structural transitions at the cytoplasmic face during integrin activation. *Proc. Natl. Acad. Sci. USA.* 101:4094–4099.

Wayner, E.A., S.G. Gil, G.F. Murphy, M.S. Wilke, and W.G. Carter. 1993. Epiligrin, a component of epithelial basement membranes, is an adhesive ligand for α3 β1 positive T lymphocytes. *J. Cell Biol.* 121:1141–1152.

Weigert, R., A.C. Yeung, J. Li, and J.G. Donaldson. 2004. Rab22a regulates the recycling of membrane proteins internalized independently of clathrin. *Mol. Biol. Cell.* 15:3758–3770.

Wilcke, M., L. Johannes, T. Galli, V. Mayau, B. Goud, and J. Salamero. 2000. Rab11 regulates the compartmentalization of early endosomes required for efficient transport from early endosomes to the trans-Golgi network. *J. Cell Biol.* 151:1207–1220.

Woods, A.J., D.P. White, P.T. Caswell, and J.C. Norman. 2004. PKD1/PKCmicro promotes alphavbeta3 integrin recycling and delivery to nascent focal adhesions. *EMBO J.* 23:2531–2543.

Zerial, M., and H. McBride. 2001. Rab proteins as membrane organizers. *Nat. Rev. Mol. Cell Biol.* 2:107–117.

Zhang, H., J.S. Berg, Z. Li, Y. Wang, P. Lang, A.D. Sousa, A. Bhaskar, R.E. Cheney, and S. Stromblad. 2004. Myosin-X provides a motor-based link between integrins and the cytoskeleton. *Nat. Cell Biol.* 6:523–531.